Journal of Photochemistry & Photobiology, A: Chemistry 444 (2023) 114996

Contents lists available at ScienceDirect

Journal of Photochemistry & Photobiology, A: Chemistry

journal homepage: www.elsevier.com/locate/jphotochem

Interaction and inhibition of lysozyme amyloid fibrillation by benzophenanthridine alkaloid sanguinarine: Photophysical, molecular docking and imaging studies

Anirban Basu [a,*], Shukdeb Sing [a], Arindam Das [a], Gouranga Jana [a], Boby Samai [b]

[a] Department of Chemistry, Vidyasagar University, Midnapore 721 102, India
[b] Department of Science and Humanities, Hooghly Institute of Technology, Hooghly 712 103, India

ARTICLE INFO

Keywords:
Sanguinarine
Lysozyme
Quenching
Docking
Fibrillation

ABSTRACT

Protein misfolding lead to pathological amyloid aggregates causing neurodegenerative disorders. Interaction and effect of benzophenanthridine alkaloid, sanguinarine (SNR hereafter), on lysozyme fibrillation was studied in the quest for designing potent antiamyloidogenics. SNR quenched the intrinsic fluorescence of lysozyme and the quenching mechanism was static. There existed one type of binding site for SNR on lysozyme and TRP residues were mainly involved in binding. 3D-fluorescence studies indicated conformational changes in lysozyme upon complexation with SNR. The binding between lysozyme and SNR was also studied by molecular docking to understand the forces involved in the binding. Effect of SNR on lysozyme fibrillation was examined from Thioflavin T assay which revealed that SNR suppressed the fibrillation of lysozyme significantly. Nile red and ANS assay revealed that SNR arrested the fibrillation. FTIR and circular dichroism showed that β-sheet content of the fibrillar species was reduced by SNR implying fibrillogenesis was inhibited as amyloid fibrils have β-sheet rich structures. AFM also revealed that SNR induced a marked decrease in the fibrillar quantity. These results can be utilized for designing potential drugs for amyloidosis.

1. Introduction

Misfolding, aggregation and pathological deposition of proteins cause fatal diseases called amyloidoses. It is marked by long dense amyloid fibrils [1]. Many human peptides and proteins have been reported to be associated with pathological amyloid aggregates [2]. Inspite of having little structural and sequential similarities, they form amyloid fibrils which has similar fibrillar morphology and other biochemical properties [3,4]. Unfolding of the protiens and their aggregation starts with destabilization of its native conformation resulting in partially unfolded intermediates [5–8]. So, inhibition of fibrillation or rupture of existing fibrillar structures is an useful therapeutic approach for the remedial treatment of amyloidosis [5,9–12]. One strategy to reduce amyloidosis is to use small natural or synthesized compounds as aggregation inhibitors. Chicken egg-white lysozyme (CEWL hereafter) is homologous to human lysozyme and its amyloidogenic variants is seen to correlate with the occurence of systemic amyloidosis [13]. The core structure called the CEWL K peptide (GILQINSRW, residues 54–62 in the β-domain of the cleft), can self-assemble and fibrillate [14,15]. In livers and kidneys human lysozyme mutants can form large amyloid deposits [16]. Lysozymes from different sources form amyloid aggregates under destabilizing conditions [17–19]. No clinical treatments are known for preventing or reversing the amyloid fibrillation. Small molecules can inhibit amyloidogenesis [20,21–25] but knowledge on the precise mechanism of inhibitory action, their effect on different kinetic aggregation parameters and unfolding pathway are still being explored [26]. Natural products, particularly the alkaloids represent an attractive pool of compounds with diverse medicinal properties which can be developed as potential therapeutic agents for amyloid related diseases [27]. Among the alkaloids, the benzophenanthridines are an interesting class of molecules having multiple pharmacological properties [28–33]. The premier benzophenanthridine alkaloid SNR (Fig. 1) has diverse medicinal applications but its antiamyloidogenic potential is still not studied [28,30,31,34–42]. Thus, in our quest to design viable antiamyloidogenic agents we have probed the interaction and influence of the benzophenanthridine alkaloid, SNR, on lysozyme fibrillogenesis using multiple biophysical assays.

* Corresponding author.
E-mail address: basu.ani.anirban@gmail.com (A. Basu).

https://doi.org/10.1016/j.jphotochem.2023.114996
Received 23 March 2023; Received in revised form 22 June 2023; Accepted 1 July 2023
Available online 3 July 2023

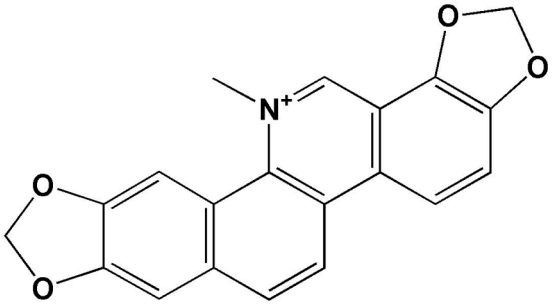

Fig. 1. Molecular structure of SNR.

2. Materials and methods

2.1. Materials

CEWL (CAS Number: L6876), SNR (CAS Number: 5578-73-4), Thioflavin T (ThT), Congo Red (CR), Nile Red (NR) and 8-Anilino-1-naphthalenesulfonic acid (ANS) were purchased from Sigma-Aldrich Corporation (St. Louis, MO, USA). 50 mM glycine-HCl buffer pH (~2.20) containing 100 mM NaCl and 1.54 mM NaN_3 was used for all the experiments. The components used for buffer preparation were of analytical grade.

2.2. Methods

Steady state fluorescence experiments were performed on a Hitachi F–7100 or Shimadzu RF-5301 PC (Shimadzu Corporation, Kyoto, Japan) spectrofluorimeter.

The fluorescence titration experiments were done keeping bandwidths of 5 nm. The excitation wavelength for CEWL was 295 nm and excitation wavelength for SNR was 470 nm. A constant concentration of CEWL (13.20 μM) was titrated with 0 μM to 33.60 μM concentrations of SNR while in another experiment 12 μM of SNR was titrated with 0 μM to 19.89 μM CEWL. After inner-filter effect correction [43,44], the quenching constant was envisaged using the Stern - Volmer equation [45],

$$\frac{F_o}{F} = 1 + K_q\tau_0[Q] = 1 + K_{sv}[Q] \tag{1}$$

where F_0 and F are the CEWL fluorescence intensities in absence and presence of SNR, respectively. K_q and τ_0 are the equilibrium quenching constants and average life time of CEWL, respectively. K_{SV} and [Q] are the Stern-Volmer quenching constant and concentration of SNR, respectively.

Fluorescence lifetime decay values were measured in Horiba DeltaFlex™ Modular Fluorescence Lifetime System (Horiba Yvon, Glasgow, UK) at excitation and emission wavelengths of 288 nm and 338 nm, respectively. The lifetime decay data were evaluated using the equation [46],

$$F(t) = \Sigma\alpha_i \exp\left(-\frac{t}{\tau_i}\right) \tag{2}$$

where F(t) = fluorescence intensity at time t and α_i is the pre-exponential factor of i^{th} time constant. For multiexponential experimental decay τ_{avg} is given by the equation [47,48],

$$\tau_{avg} = \sum a_i\tau_i \tag{3}$$

here, τ_i denote the fluorescence life time and α_i is the relative amplitude, respectively.

The CEWL-SNR binding constant (K_A) and the number of binding sites (n) were subsequently derived from the equation [49–51],

$$\log\frac{(F_0 - F)}{F} = \log K_A + n\log[Q] \tag{4}$$

here, K_A = CEWL-SNR equilibrium binding constant and 'n' represents the binding sites on CEWL. K_A and n were determined from the intercept and slope of the linear graph of $\log\frac{(F_0-F)}{F}$ *vs* log[Q].

3D-fluorescence spectra of CEWL (3.4 μM) in presence and absence of SNR (24 μM) were obtained by the analysis of emission (220 to 450 nm) and excitation (200 to 400 nm) spectral range with 5 nm increment. The data is average of 15 scans.

200 mg of CEWL was dissolved in glycine-HCl buffer (20 ml). To prepare CEWL fibrils 2 ml stock CEWL solution was diluted five folds with the buffer and agitated (580 rpm) at 60 °C for 6 h [52–54]. A similar solution with 50 μM SNR was also prepared which was also stirred (580 rpm) at 60 °C for 6 h. 0.75 ml aliquots were withdrawn from both the solutions at 30 mim intervals for 6 h and stored carefully for monitoring the fibrillation kinetics by ThT assay and other related experiments.

For ThT assay a stock solution of ThT was prepared. 75 μl aliquots withdrawn at varying time interval were diluted with 675 μl buffer. Then appropriate volumes of stock ThT solution was added to it and stored for 1 h. Fluorescence at 485 nm were measured by exciting the samples at 440 nm and after inner filter effect corrections [43,44] the inhibitory effect of various SNR concentrations on CEWL fibrillation was determined from the percentage of ThT fluorescence decrease at 6 h using the equation

$$\%decreaseinThTfluorescence = \frac{F_o - F}{F_o} \times 100\% \tag{5}$$

where, F_o and F are ThT fluorescence of CEWL samples in absence and presence of SNR.

The kinetics of fibrillation was analyzed using the equation [55]

$$F = F_{min} + \left(\frac{F_{max} - F_{min}}{1 + e^{[\{t-t_0\}/k]}}\right) \tag{6}$$

where F, F_{min} and F_{max} are fluorescence at time t, initially and after saturation, respectively. t and t_0 are incubation time and time to reach half of the maximum fluorescence while k is first order aggregation constant. Apparent growth rate constant (k_{app}) is given by $1/k$. All the data reported are average of four independent determinations.

For NR assay 1 mM solution of NR in DMSO was prepared. 50 μl of the CEWL samples were diluted to 750 μl with buffer. NR solution was then added so as to keep the final concentration at 1 μM. It was stored for 30 mins, then fluorescence at emission maxima were noted by exciting at 550 nm.

For ANS assay a stock solution of ANS was prepared and 50 μl of CEWL sample solutions were diluted to 750 μl. Then the stock ANS solution was added so that ANS concentration was 25 μM. Fluorescence spectra were taken after exciting at 370 nm.

Using the Parkin Elmer's FTIR spectrophotometer decorated with Zinc Selenide (ZnSe) for Attenuated Total Reflectance (ATR), KBr beam splitter and $LiTaO_3$ detector (Perkin Elmer, USA) the secondary structural changes in CEWL upon fibrillation both in the absence and presence of SNR was investigated.

100 μl of CEWL samples were diluted to 300 μl and far-UV circular dichroism (CD) was recorded on Jasco J815 spectrometer [49]. Secondary structure of CEWL was measured using "CONTINLL" program of DICHROWEB (dataset 4 was the reference set) [56–60].

Atomic force microscopy (AFM) imaging studies were done according to the protocols described in details earlier [61–63]. CEWL solutions were diluted 200 folds, 5 μl of the solution was placed on freshly cleaved mica and dried before imaging. AFM images were processed with Picoview 1.1 version software.

2.3. Statistical analysis

The data are represented as mean ± standard deviation (S.D.) of four independent determinations.

3. Results and discussion

3.1. Spectrofluorimetric studies

Fluorescence gives detailed information about CEWL fluorophores which are very sensitive to the surrounding polarity and ability of CEWL to bind with SNR [49,64]. SNR quenched the intrinsic fluorescence of CEWL which gives information about that the nature and binding mode. Tryptophan (TRP) 62 and 63 are more exposed towards the solvent. The TRP residue at position 63 is not buried in the hydrophobic core, it is lying in the active site hinge region. On the other hand, the TRP 62 is exposed to the solvents [65]. Information about the changes in the local environment of these residues upon SNR binding (TRP-62, TRP-63) can be obtained through fluorescence quenching studies [66]. CEWL was excited at 295 nm and the emission maximum was around 338 nm.

In Fig. 2A we can see the emission spectral change of CEWL in presence of SNR. The intrinsic fluorescence spectra of CEWL were sufficiently quenched (78%) by SNR with a marked red shift of about 23 nm. After certain time, these effects reached a saturation point.

The K_{SV} value was estimated to be $(4.57 \pm 0.12) \times 10^4$ at 25 °C using equation (1) after inner filter effect correction. Furthermore, the K_{SV} values were determined at 20, 30 and 35 °C. The K_{SV} values were found to decrease gradually on increasing the temperature from 20 to 25 to 30 to 35 °C, suggesting a static quenching mechanism which was independently verified by fluorescence lifetime experiment.

SNR also has a fluorophore that exhibit emission maxima at 584 nm when excited at 470 nm. The fluorescence changes of SNR upon adding CEWL is presented in Fig. 2B.

After successive additions of CEWL the fluorescence of SNR reached a saturated point and further addition of CEWL did not cause any change.

Further knowledge about the microenvironment of the fluorophores and the binding interaction between SNR and CEWL was studied from time-resolved fluorescence experiment. The fluorescence lifetime study is most effective to analyze the quenching mechanism (static or dynamic). The time resolved fluorescence decay profiles of CEWL in presence and absence of SNR (Fig. 3) were analyzed and the average lifetime value of CEWL was 1.096 ns whereas that of CEWL-SNR complex was 1.074 ns which supported the fact that the mechanism of quenching process was static in nature and due to the formation of ground state complex between CEWL and SNR because in case of dynamic quenching the fluorescence lifetime value significantly changes [46].

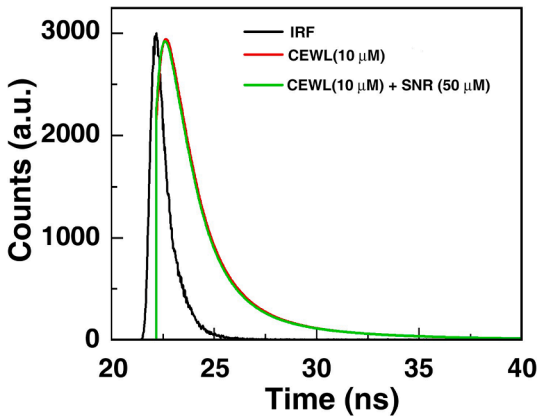

Fig. 3. Time-resolved fluorescence decay profile of CEWL and its complex with SNR.

From the above fluorescence lifetime studies we can assume that the specific binding interaction occurred between SNR and CEWL leading to ground state complexation. Therefore, SNR can bind independently to identical site of CEWL.

K_A was $(5.22 + 0.17) \times 10^4\ M^{-1}$, which suggested moderate binding interaction. We obtained the binding sites from the value of '***n***' and it is almost unity indicating that one type of binding site exists and TRP residues are mainly involved in binding.

3D-excitation-emission matrix analysis gives additional information about conformational changes of CEWL upon binding of SNR [67,68]. The 3D-excitation-emission spectrum and the contour form of CEWL in presence and absence of SNR is presented in Fig. 4. In Fig. 4 peak 1 ($\Delta\lambda_{ex}$ = 280 and and $\Delta\lambda_{em}$ = 337 nm) and peak 'a' ($\Delta\lambda_{ex} = \Delta\lambda_{em}$) is mainly expressed due to the fluorescence excitation-emission spectrum of TRP and tyrosine residues of CEWL and 1st order Rayleigh scattering ($\lambda_{ex} = \lambda_{em}$), respectively [69]. After successive addition of SNR to CEWL we observed that the Stokes shift ($\Delta\lambda$) increased from 57 to 84 nm and the intrinsic fluorescence intensity decreased.

This suggested that the less polar region and the TRP and tyrosine residues of CEWL inserted into the hydrophobic cavity were exposed due to SNR-CEWL binding. The increase in Stokes shift value indicated the conformational change of CEWL. We have another fluorescence peak 2 ($\Delta\lambda_{ex}$ = 225 and $\Delta\lambda_{em}$ = 339 nm) due to the n → π* transition in

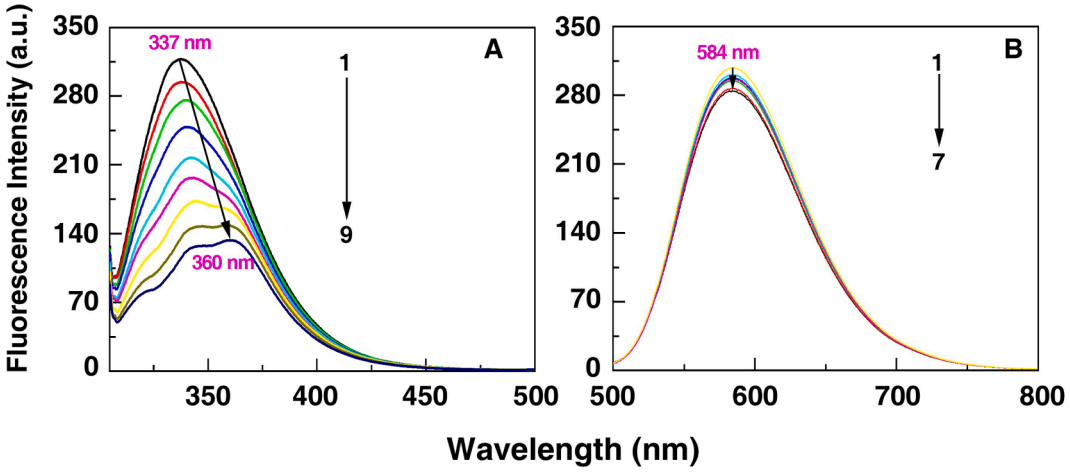

Fig. 2. Fluorescence spectra of (**A**) CEWL (13.20 μM) treated with 0 to 33.60 μM SNR (curves 1–9) and (**B**) SNR (12 μM) treated with 0 to 19.89 μM CEWL (curves 1–7).

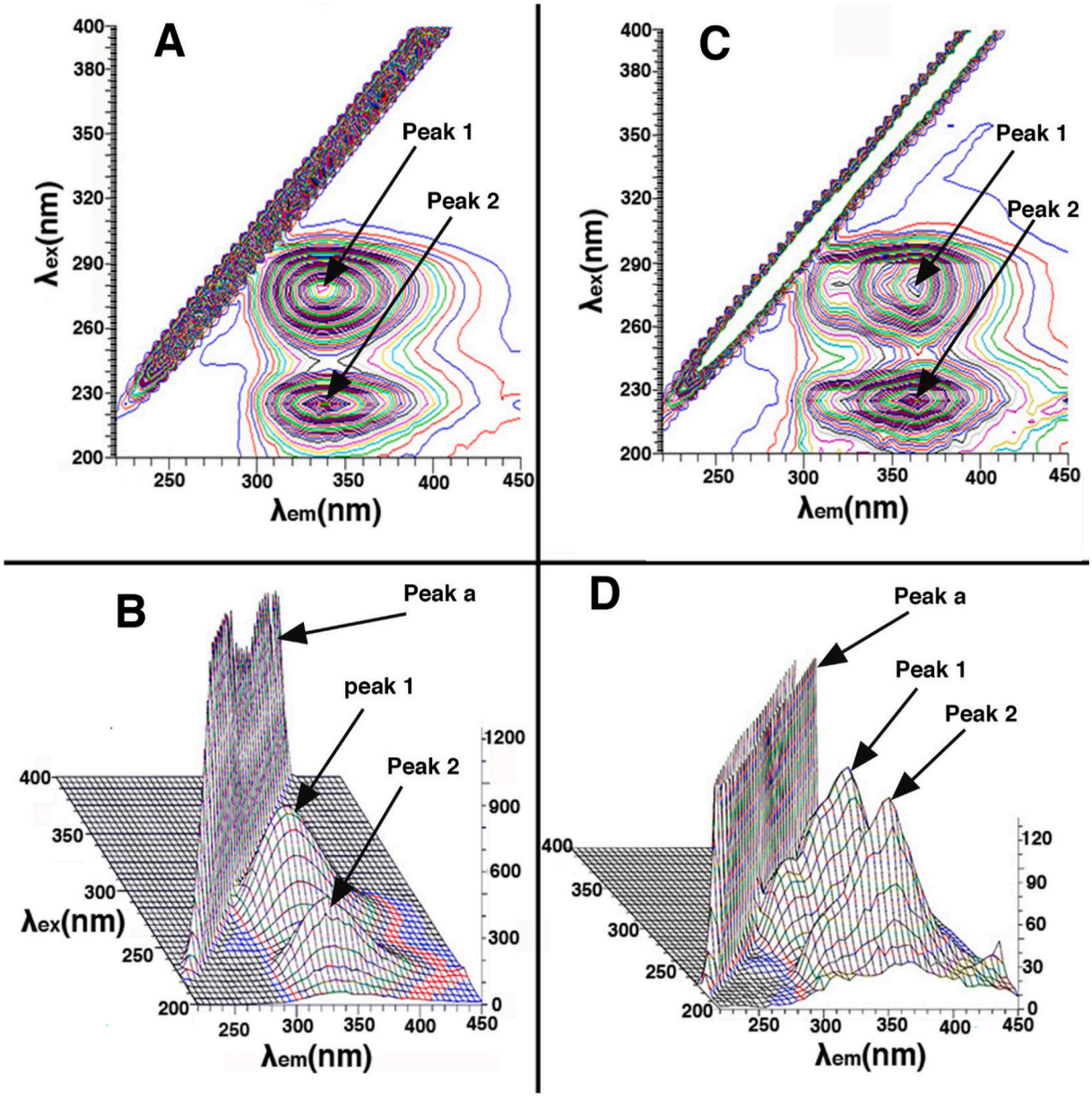

Fig. 4. 3D-fluorescence spectra of CEWL (A & B) (3.40 μM) and CEWL-SNR (C & D) (24 μM) system.

polypeptide backbone. SNR induced conformational change and shift of CEWL amino acid residues from hydrophobic to hydrophilic environment, i.e, non-polar to polar region.

3.2. Molecular docking studies

In silico investigation of binding interaction between CEWL and SNR was performed using Autodock at RMSD tolerance of 2 Å. SNR has no active torsion because it does not contain any rotatable bond. The binding Gibbs free energy ($\Delta G_{binding}$) of each conformation was calculated using the equation [70].

$$\Delta G_{\text{binding}} = \Delta G_{\text{vdW}} + \Delta G_{\text{elec}} + \Delta G_{\text{H-bond}} + \Delta G_{\text{desolv}} + \Delta G_{\text{tors}} \quad (7)$$

where ΔG_{vdW}, ΔG_{elec}, $\Delta G_{\text{H-bond}}$, ΔG_{desolv} and ΔG_{tors} are the free energy changes due to Van der waal's interaction, electrostatic interaction, H-bonding, desolvation and torsional degree of freedom, respectively.

Lowest binding energy between CEWL and SNR was found to be −6.12 kcal/mol over 100 probable conformations generated from docking result using two PDB ID. Best conformers clearly indicate that SNR interact in big enzymatic cavity of CEWL and make different types of interaction (Fig. 5A). Binding energy and interaction type with distance of best interacting conformer of each PDB ID is given in Table 1. In best docking conformation there are two conventional H-bonds between SNR and ASN 59 & ARG 61 residue of CEWL with distance 2.30 Å and 1.81 Å, respectively. Besides, conventional hydrogen bond, some non-classical H-bond such as carbon-hydrogen bond and π-donor hydrogen bonds was also found in docking study. TRP 62 makes a π-cationic interaction with aromatic π-electron cloud of SNR. In addition to these interactions other hydrophobic interactions like π-π stacked, π-π T-shaped, π alkyl and alkyl are also present. The visualization of docking data on both 3D (Fig. 5B & C) and 2D (Fig. 6) indicate that binding of SNR with CEWL is not hydrophobic exclusively but there are other interactions such as conventional H-bond, π-cationic dipolar interaction, π donor H-bond etc.

Change in accessible surface area to solvent was calculated using following equation

$$\Delta ASA = ASA_{CEWL} - ASA_{CEWL-SNRcomplex} \quad (8)$$

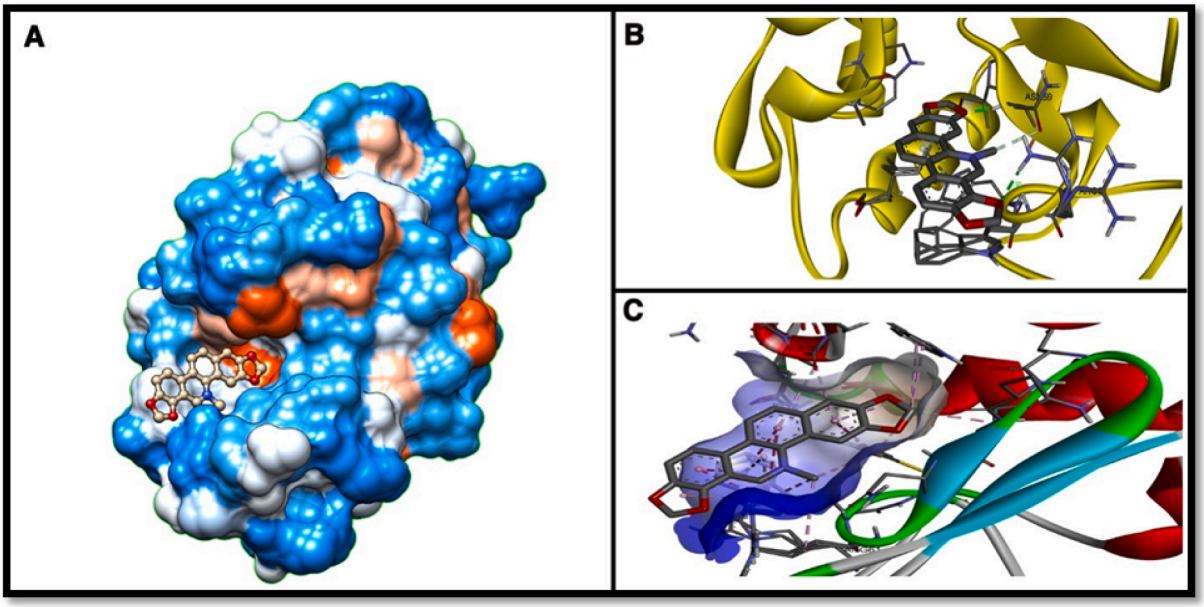

Fig. 5. (A) 3D placement of SNR in enzymatic cavity of CEWL along with (B) H-bonding and (C) Hydrophobic interaction.

Table 1
Binding parameters of the interactions between PDB entries of CEWL and SNR obtained through molecular docking.

PDB ID	Gibbs free energy (kcal/mol)	Inhibition constant(μM)	H bond making residues	Hydrophobic interacting residues
2vb1	−6.12	32.42	ASN 59, ARG 61	ILE 58, TRP 62, TRP 63, ILE 98, ALA 107 and TRP 108
2ydg	−5.88	49.4	–	TRP 62, TRP 63, ILE 98, ALA 107 and TRP 108

ΔASA of each residue of more stable conformer with lowest binding energy was calculated in $Å^2$ and significant changes are given in Table 2. Reduction of ASA of CEWL-SNR complex in comparison to CEWL suggests that some solvent accessible area of CEWL was captured by SNR due to its close proximity to CEWL during the binding reaction. Location of residues enlisted in Table 2 also confirmed that SNR bind at the enzymatic cavity of CEWL.

3.3. ThT assay

ThT is a fluorescent dye used for detecting β-sheet structures. So, ThT fluorescence was measured to monitor CEWL fibrillation and whether SNR can suppress the fibrillation kinetics. Fluorescence intensity of ThT is weak in aqueous acidic medium but it increases on binding with linear

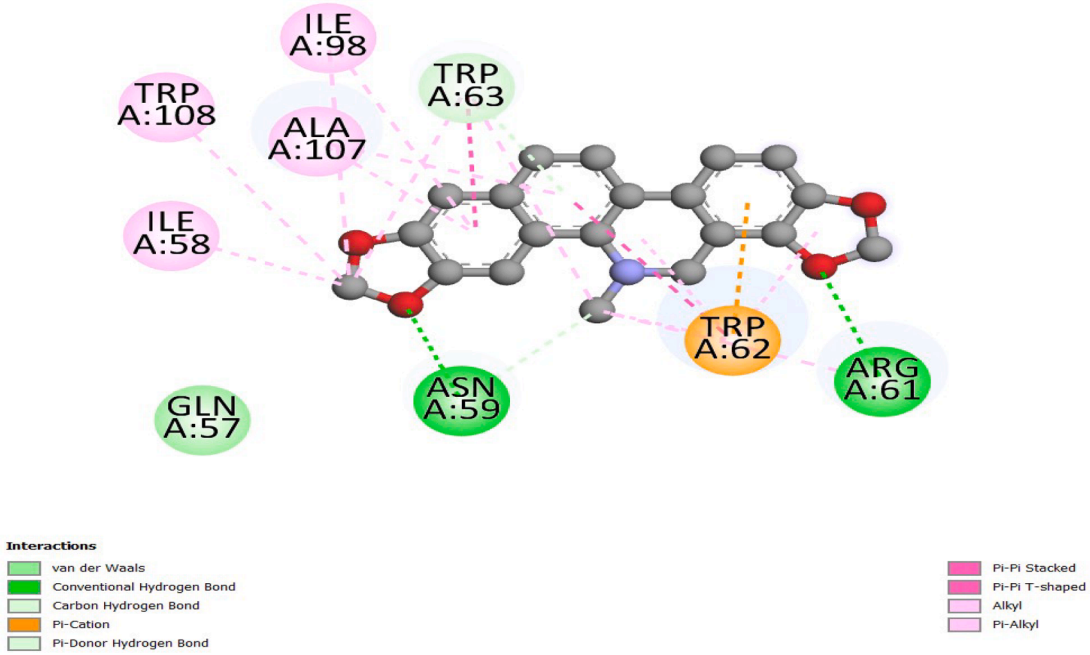

Fig. 6. 2D image of interaction of most stable conformation of CEWL with SNR.

Table 2
ASA value of CEWL, CEWL-SNR complex and change in ASA during CEWL-SNR complexation.

Residue		ASA $_{CEWL}$ (Å^2)	ASA $_{CEWL\text{-}SNR\ complex}$ (Å^2)	ΔASA (Å^2)
23	TYR	48.199	38.498	9.701
34	PHE	67.317	58.459	8.858
53	TYR	15.124	11.139	3.985
57	GLN	21.546	17.543	4.003
58	ILE	4.313	0.227	4.086
59	ASN	40.393	10.762	29.631
61	ARG	73.426	52.369	21.057
62	TRP	104.391	39.923	64.468
63	TRP	15.147	0.207	14.94
73	ARG	134.574	128.723	5.851
75	LEU	68.398	61.837	6.561
76	CYS	18.127	16.538	1.589
84	LEU	52.547	43.388	9.159
89	THR	52.9	46.602	6.298
90	ALA	19.539	17.104	2.435
98	ILE	2.837	0	2.837
99	VAL	9.935	1.856	8.079
100	SER	53.235	46.345	6.89
102	GLY	74.072	65.658	8.414
103	ASN	43.951	36.036	7.915
106	ASN	91.133	87.668	3.465
107	ALA	53.042	7.005	46.037
108	TRP	8.378	2.966	5.412

array of fibrils [71]. The ThT fluorescence of CEWL fibrils in absence of SNR was significantly higher than those in presence of SNR. Addition of SNR resulted in inhibition of CEWL fibrillation. Compared to the CEWL samples without SNR, increase in ThT fluorescence of CEWL samples treated with SNR was significantly less. At 15, 30 and 50 μM concentrations of SNR the ThT fluorescence of CEWL fibrils was reduced by (34.70 ± 3.15), (48.50 ± 3.52) and (63.84 ± 4.75)%, respectively, after 6 h. Thus, the extent of inhibition enhanced with increasing SNR concentration. Thereafter, at 55 and 60 μM SNR concentration only small variations in extent of fibrillation was observed (Fig. 7). Hence, the subsequent assays have been performed keeping an optimum SNR concentration of 50 μM.

The ThT fluorescence for CEWL samples followed a nucleation-dependent pathway. ThT fibril formation profiles of CEWL samples is shown in Fig. 8 which revealed that ThT fluorescence of CEWL samples alone increased significantly after 1 hr of incubation followed by saturation phase. The variation of ThT fluorescence against time was sigmoidal with a lag phase when the critical nuclei are formed followed by a growth phase where the fluorescence enhanced rapidly and finally a saturation phase. The apparent growth rate constant of the fibrils were estimated to be (8.22 ± 0.04) and (7.32 ± 0.03) h^{-1}, respectively, in the absence and presence of SNR.

The decrease in ThT fluorescence in presence of SNR can be explained on basis of the non-covalent inhibitory interaction between SNR and aggregation-prone partially unfolded form of CEWL formed initially. The aromatic chromophore of SNR along with its methylene

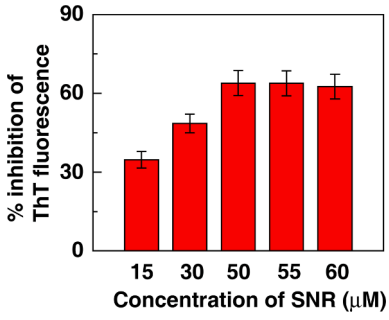

Fig. 7. Percentage of inhibition of ThT fluorescence intensity of CEWL fibrils at 485 nm in presence of 15, 30, 50, 55 and 60 μM SNR.

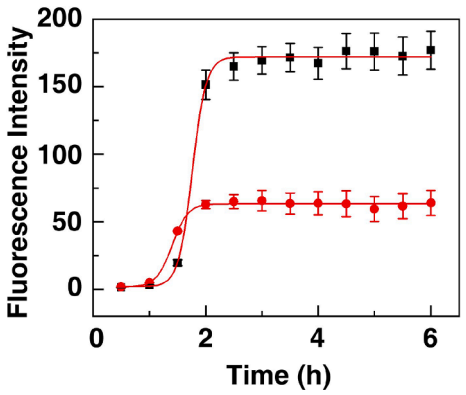

Fig. 8. Variation of the ThT fluorescence intensity at 485 nm with time for CEWL samples in absence (■) and presence (•) of 50 μM SNR.

dioxy groups provides a template for SNR-CEWL complexation through π-stacking, hydrogen bonding, van der Waals and hydrophobic interactions which inhibit the hydrophobic regions in the partially unfolded CEWL to interact resulting in the reduction of aggregation propensity of partially unfolded CEWL which leads to suppression of fibrillation ultimately. Such inhibition of fibrillation due to different non-covalent interactions between small molecules and proteins has also been reported previously [72–74].

3.4. NR assay

Effect of fibrillation on the CEWL tertiary structure was determined by examining the NR fluorescence emission with time. NR is a lipophilic fluorescent dye for studying the microenvironmental changes in biomacromolecules [52,75]. Fluorescence of NR is related to CEWL surface hydrophobicity. In Fig. 9 changes in NR emission spectra is shown before and after fibrillation. CEWL samples stained with NR were weakly fluorescent before fibrillation but there was increase in fluorescence of CEWL samples after fibrillation which indicates change in CEWL surface hydrophobicity upon fibrillation.

CEWL samples treated with SNR showed comparatively less enhancement in fluorescence indicating that surface hydrophobicity and microenvironmental changes in CEWL are arrested by SNR. So, tertiary structural changes in CEWL were arrested in presence of SNR. As surface hydrophobicity and tertiary structural changes occur upon fibrillation therefore we can say that fibrillation is suppressed by SNR. There was also a blue-shift in NR emission maximum before the enhancement in fluorescence from 664 to 616 nm which indicates the exposure of buried hydrophobic clusters. The NR emission maxima is even more sensitive to tertiary structural changes in CEWL than the fluorescence.

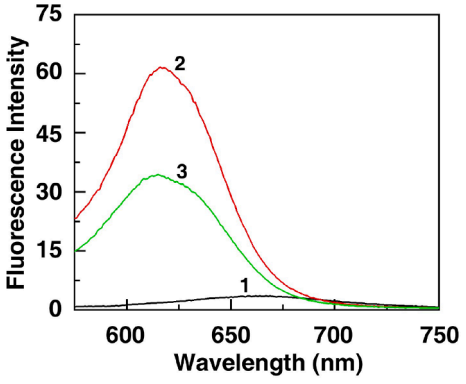

Fig. 9. NR fluorescence spectra of CEWL samples before (curve 1) & after fibrillation (curves 2 and 3). Curves 2 and 3 represent the NR fluorescence spectra of CEWL in absence and presence of 50 μM SNR, respectively.

3.5. ANS binding assay

ANS being a fluorescent probe which binds to hydrophobic regions of CEWL can detect the partially unfolded state of CEWL. Before aggregation certain conformational changes occur in CEWL which results in the exposure of non-polar surface area.

Exposure of initially buried hydrophobic patches of CEWL is a key step in the fibrillation. Therefore, changes in the hydrophobic regions is used for monitoring fibrillation [73,76–78]. Fig. 10 depicts the ANS fluorescence of CEWL before and after fibrillation both in absence and presence of SNR. It has weak fluorescence in aqueous acidic buffer but in presence of fibrils the ANS fluorescence enhances remarkably with blue shift of maxima to 480 nm suggesting the complexation of ANS with exposed hydrophobic regions of CEWL. However, SNR caused the ANS fluorescence to be decreased by 47% at 480 nm. This drastic reduction in ANS fluorescence indicated lesser exposure of hydrophobic regions of CEWL leading to lesser degree of complexation between ANS and the hydrophobic patches of CEWL. As hydrophobic patches of CEWL are exposed during fibril formation therefore a reduction in exposure of non-polar regions suggest SNR induced a reduction in the extent of CEWL fibrillation.

3.6. FTIR analysis

The characterization of the secondary structure of CEWL fibrils in the absence and presence of SNR can be accomplished using FTIR spectroscopy. Secondary structure of CEWL was investigated using the amide I, II and III FTIR spectral bands in the region 1800–1300 cm^{-1}, which are derived from the polypeptide backbone's vibrational modes. The amide I band (1600–1700 cm^{-1}) which is most frequently used to evaluate the secondary structure of proteins arises due to the sensitivity of C = O bond stretching vibration. The N-H bending combined with –CN stretching and –NH bending are responsible for amide II and amide III bands, respectively. The amide I band is made up of various assignments like β-sheet within 1610–1635 cm^{-1}; random coil within 1630–1645 cm^{-1}; alpha helix within 1648–1660 cm^{-1}; antiparallel β-sheet and β-turn within 1665–1695 cm^{-1} [79–81].

From Fig. S1 it is evident that native CEWL has sharp peak at 1648 cm^{-1} which indicate α-helical conformation of CEWL. After CEWL fibril formation the peak position shifted to 1628 cm^{-1}, which suggested the formation of β-sheet rich conformation. In presence of SNR a lower absorbance at 1628 cm^{-1} was observed compared to the CEWL fibrils not treated with SNR, which indicated loss of β-sheet rich fibrillar conformation [82].

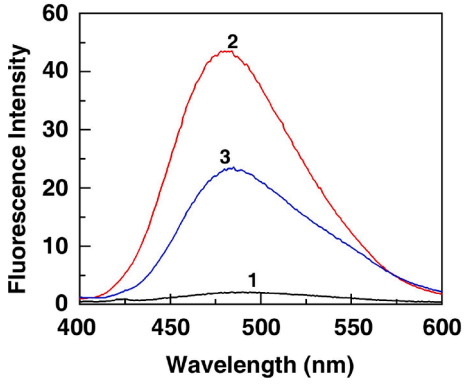

Fig. 10. ANS fluorescence of CEWL samples before (curve 1) & after fibrillation (curves 2 and 3). Curves 2 & 3 represent the ANS fluorescence spectra of CEWL in absence and presence of 50 μM SNR, respectively.

3.7. CD studies

Conformational changes in CEWL upon fibrillation were studied from far-UV CD spectra. Prior to fibrillation CEWL exhibited minima at 208 and negative shoulder at 223 nm which are the characteristics of α-helical structure (Fig. S2) [83,84]. However, upon fibrillation the far-UV CD spectrum of CEWL changed to a highly amyloidogenic β-sheet rich conformation with a minimum at 221 nm (Fig. S2). The β-sheet content of CEWL enhanced from (13.70 ± 1.65) to (63.10 ± 4.77)% upon fibrillation. In presence of SNR the β-sheet content was significantly reduced to (48.80 ± 3.17)%. The change in β-sheet content of CEWL before and after fibrillation is depicted in Fig. 11. This decrease in β-sheet content suggests inhibition of fibrillation by SNR as α-to-β transition with increase in β-sheet content is the hallmark of fibrillogenesis.

3.8. AFM imaging

AFM was performed to understand the morphology of CEWL fibrils as well as to examine the fibril arresting ability of SNR. From Fig. 12A it is evident that after 6 h the CEWL samples showed large quantities of long, matured, compact and dense fibrillar structures which are typical of amyloid fibrils. Fig. 12B shows clearly that fibrillation was suppressed by SNR. Fibrils were significantly less dense and compact upon addition of SNR. From comparison of these two figures we see that after 6 h amyloid fibrillation was arrested by SNR. Fibrils were markedly lesser in quantity and sparsely populated in presence of SNR. Thus, AFM studies unequivocally establish that CEWL fibrillogenesis was inhibited by SNR.

Protein aggregation resulting in cognitive dysfunction is responsible for neurodegenerative diseases. CEWL undergoes aggregation leading to amyloid fibrillation. So, CEWL fibrillation inhibition by small molecules, nanoparticles, ionic liquids and peptides has gained eminence [52,49,55,61–63,72,85–87]. SNR has been studied as potential inhibitor of amyloid fibrillation due to its multiple medicinal properties [31,34–42]. Monitoring the changes in CEWL conformation early during its unfolding allow a better understanding of CEWL fibrillation and ways to arrest it by preventing CEWL to form locally unfolded intermediates. The results suggested that SNR can efficiently inhibit CEWL fibrillation by complexing with CEWL. The reduction in ANS fluorescence is an indicator of a lesser hydrophobic core being exposed to solvent, suggesting that SNR stabilizes conformation of CEWL even when exposed to fibrillation conditions. SNR binds with CEWL molecules and glues the aggregation-prone region of the β-domain with the α-domain causing reduction in the β-domain unfolded intermediates which results in the suppression of fibrillation [73,88]. Several azo dyes like amaranth, tartrazine, carmoisine, fast green FCF, sunset yellow and ponceau 4R have been reported to possess excellent antifibrillation potential against CEWL but their use as antiamyloidogenic agents is restricted due to their potential toxicity [49,61,84,89]. Amaramth (25 μM), carmosine (50 μM)

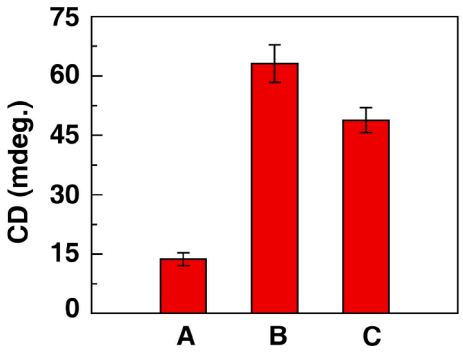

Fig. 11. Content of β-sheet of CEWL (A) before & after fibrillation in the (B) absence and (C) presence of SNR.

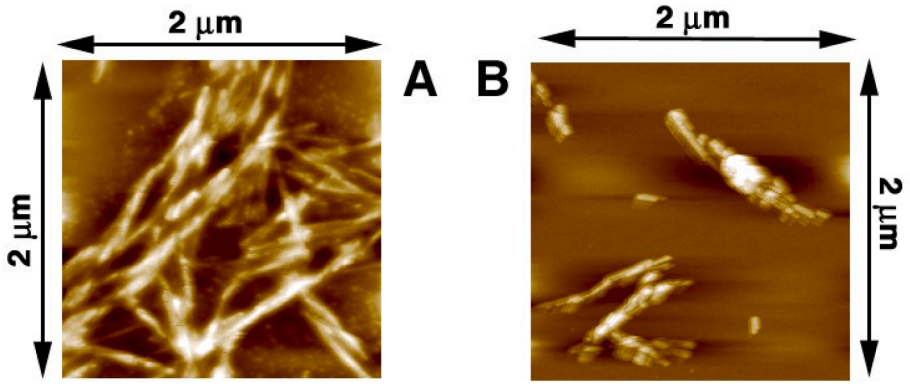

Fig. 12. AFM images of CEWL fibrils (A) formed alone & (B) in presence of SNR after 6 h.

and tartrazine (100 μM) inhibited fibrillation by 47, 81 and 73%, respectively. Other dyes like toluidine blue O and methylene blue has also shown inhibitory effects on lysozyme fibrillation [90]. Polyphenols like quercetin, myricetin, morin, luteolin, kaempferol, curcumin and EGCG have also been reported to possess significant inhibitory effect towards lysozyme fibrillation [15,16,88,91,92]. Curcumin is reported to suppress fibrillation completely at 200 μM and EGCG suppresses fibrillation by 70% at 400 μM [92] whereas SNR suppressed fibrillation by around 64% at relatively lower concentration (50 μM). Wu et al. reported that carnoisine, an eye-drop component for treatment and prevention of senile cataract, exhibited its antiamyloidogenicity in millimolar concentration range [52]. Thus, SNR appears to possess much higher antiamyloidogenic potential compared to carnoisine as it can arrest fibrillation effectively in micromolar concentration range. The isoquinoline alkaloid coralyne was reported to arrest fibrillation in CEWL by 97% at 25 μM concentration [63]. So, it is an even more potent inhibitor of fibrillation than SNR.

4. Conclusions

Interaction and effect of SNR on amyloid fibrillation in CEWL has been studied. There was ground state complexation between SNR and CEWL which resulted in exposure of the buried amino residues of CEWL to a hydrophilic environment. 3D-fluorescence studies revealed SNR binding caused conformational changes in CEWL. Molecular docking study reveals effective binding of SNR at enzymatic site of CEWL. SNR suppressed CEWL fibrillar assembly formation markedly as revealed by ThT assay. NR and ANS assay testified that CEWL surface hyrdophobicity changes along with exposure of hydrophobic regions upon fibrillation were suppressed efficiently by SNR. β-sheet content of CEWL increases upon fibrillation but SNR affected significant reduction in the β-sheet content of CEWL suggesting SNR had an inhibitory effect on the fibrillation. AFM imaging showed that quantity of fibrils was markedly reduced by SNR. Thus, we conclude SNR attenuated CEWL fibrillogenesis which provides a model for exploring the inhibitory effects of alkaloids on protein fibrillation in vitro. As the inhibitory effect was observed in micromolar concentration range so such compounds having minimal toxicity can be studied for their potential antiamyloidogenic effects for the development of amyloid related therapeutics.

CRediT authorship contribution statement

Anirban Basu: Conceptualization, Funding acquisition, Investigation, Writing – original draft, Writing – review & editing, Validation, Formal Analysis, Resources. **Shukdeb Sing:** Investigation, Formal Analysis, Writing – original draft, Writing – review & editing, Validation. **Arindam Das:** Investigation, Formal Analysis, Writing – original draft, Writing – review & editing. **Gouranga Jana:** Investigation, Writing – original draft, Writing – review & editing. **Boby Samai:** Formal Analysis, Writing – original draft.

Declaration of Competing Interest

The authors declare that they have no known competing financial interests or personal relationships that could have appeared to influence the work reported in this paper.

Data availability

Data will be made available on request.

Acknowledgements

AB and GJ thanks Department of Science and Technology and Biotechnology, Govt. of West Bengal (GO No.: 32(Sanc.)-ST/P/S&T/15G-13/2018 dated 31.01.2019) for providing financial assistance. AB also acknowledges the financial assistance from DST FIST, Govt. of India (Sanction letter No. SR/FST/CS-I/2017/7(C) dated December 28, 2018). SS is a recipient of JRF (NET) from UGC, Govt. of India.

Appendix A. Supplementary data

Supplementary data to this article can be found online at https://doi.org/10.1016/j.jphotochem.2023.114996.

References

[1] F. Chiti, C.M. Dobson, Protein misfolding, functional amyloid and human disease, Ann. Rev. Biochem. 75 (1) (2006) 333–366.
[2] S.-S. Wang, Y.-T. Hung, W.-S. Wen, K.-C. Lin, G.-Y. Chen, Exploring the inhibitory activity of short-chain phospholipids against amyloid fibrillogenesis of hen egg-white lysozyme, Biochim. Biophys. Acta. 1811 (5) (2011) 301–313.
[3] K.F. DuBay, A.P. Pawar, F. Chiti, J. Zurdo, C.M. Dobson, M. Vendruscolo, Prediction of the absolute aggregation rates of amyloidogenic polypeptide chains, J. Mol. Biol. 341 (5) (2004) 1317–1326.
[4] J. Goers, S.E. Permyakov, E.A. Permyakov, V.N. Uversky, A.L. Fink, Conformational prerequisites for alphalactalbumin fibrillation, Biochemistry 41 (2002) 12546–12551.
[5] M. Bartolini, V., Andrisano Strategies for the inhibition of protein aggregation in human diseases, ChemBioChem 11 (2010) 1018–1035.
[6] M. Bucciantini, E. Giannoni, F. Chiti, F. Baroni, L. Formigli, J. Zurdo, N. Taddei, G. Ramponi, C.M. Dobson, M. Stefani, Inherent toxicity of aggregates implies a common mechanism for protein misfolding diseases, Nature 416 (6880) (2002) 507–511.
[7] A.R. Ladiwala, J.S. Dordick, P.M. Tessier, Aromatic small molecules remodel toxic soluble oligomers of amyloid through three independent pathways, J. Biol. Chem. 286 (2001) 3209–3218.
[8] M. Sunde, L.C. Serpell, M. Bartlam, P.E. Fraser, M.B. Pepys, C.C. Blake, The common core structure of amyloid fibrils by synchrotron X-ray diffraction, J. Mol. Biol. 273 (1997) 729–739.
[9] Z. Gazova, K. Siposova, E. Kurin, P. Mučaji, M. Nagy, Amyloid aggregation of lysozyme: the synergy study of red wine polyphenols, Proteins 81 (2013) 994–1004.

[10] M. Masuda, N. Suzuki, S. Taniguchi, T. Oikawa, T. Nonaka, T. Iwatsubo, S. Hisanaga, M. Goedert, M. Hasegawa, Small molecule inhibitors of alpha-synuclein filament assembly, Biochemistry 45 (2006) 6085–6094.
[11] J.-B. Wang, Y.-M. Wang, C.-M. Zeng, Quercetin inhibits amyloid fibrillation of bovine insulin and destabilizes preformed fibrils, Biochem. Biophys. Res. Commun. 415 (4) (2011) 675–679.
[12] M. Mahdavimehr, A.A. Meratan, M. Ghobeh, A. Ghasemi, A.A. Saboury, M. Nemat-Gorgani, P. van der Wel, Inhibition of HEWL fibril formation by taxifolin: Mechanism of action, PLoS ONE 12 (11) (2017) e0187841.
[13] M.B. Pepys, G.M. Hirschfield, G.A. Tennent, J. Ruth Gallimore, M.C. Kahan, V. Bellotti, P.N. Hawkins, R.M. Myers, M.D. Smith, A. Polara, A.J.A. Cobb, S.V. Ley, J. Andrew Aquilina, C.V. Robinson, I. Sharif, G.A. Gray, C.A. Sabin, M.C. Jenvey, S. E. Kolstoe, D. Thompson, S.P. Wood, Targeting C-reactive protein for the treatment of cardiovascular disease, Nature 440 (7088) (2006) 1217–1221.
[14] Y. Sugimoto, Y. Kamada, Y. Tokunaga, H. Shinohara, M. Matsumoto, T. Kusakabe, T. Ohkuri, T. Ueda, Aggregates with lysozyme and ovalbumin show features of amyloid-like fibrils, Biochem. Cell Biol. 89 (6) (2011) 533–544.
[15] X. Chong, L. Sun, Y. Sun, L. Chang, A.K. Chang, X. Lu, X. Zhou, J. Liu, B. Zhang, G. W. Jones, J. He, Insights into the mechanism of how morin suppresses amyloid fibrillation of hen egg white lysozyme, Int.l J. Biol. Macromol. 101 (2017) 321–325.
[16] M.S. Borana, P. Mishra, R.R.S. Pissurlenkar, R.V. Hosur, B. Ahmad, Curcumin and kaempferol prevent lysozyme fibril formation by modulating aggregation kinetic parameters, Biochim. Biophys. Acta 1844 (3) (2014) 670–680.
[17] S. Raccosta, V. Martorana, M. Manno, Thermodynamic versus conformational metastabilityin fibril-forming lysozyme solutions, J. Phys. Chem. B 116 (40) (2012) 12078–12087.
[18] L.N. Arnaudov, R. de Vries, Thermally induced fibrillar aggregation of hen egg white lysozyme, Biophys. J. 88 (1) (2005) 515–526.
[19] Y. Zou, Y. Li, W. Hao, X. Hu, G. Ma, Parallel β-sheet fibril and antiparallel β-sheet oligomer: new insights into amyloid formation of hen egg white lysozyme under heat and acidic condition from FTIR spectroscopy, J. Phys. Chem. B 117 (2013) 4003–4013.
[20] R. Liu, R. Su, M. Liang, R. Huang, M. Wang, W. Qi, Z. He, Physicochemical strategies for inhibition of amyloid fibril formation: an overview of recent advances, Curr. Med. Chem. 19 (24) (2012) 4157–4174.
[21] D.E. Ehrnhoefer, J. Bieschke, A. Boeddrich, M. Herbst, L. Masino, R. Lurz, S. Engemann, A. Pastore, E.E. Wanker, EGCG redirects amyloidogenic polypeptides into unstructured, off-pathway oligomers, Nat. Struct. Mol. Biol. 15 (6) (2008) 558–566.
[22] V. Sharma, K.S. Ghosh, Inhibition of amyloid fibrillation by small molecules and nanomaterials: strategic development of pharmaceuticals against amyloidosis, Protein Pept. Lett. 26 (5) (2019) 315–323.
[23] A. Sharma, D. Kesamsetty, J. Debnath, K.S. Ghosh, Inhibition of lysozyme amyloid fibrillation by curcumin-conjugated silver nanoparticles: A multispectroscopic molecular level study, J. Mol. Liq. 372 (2023), 121156.
[24] V. Sharma, S. Sharma, S. Rana, K.S. Ghosh, Inhibition of amyloid fibrillation of human γD-crystallin by gold nanoparticles: studies at molecular level, Spectrochim. Acta A Mol. Biomol. Spectrosc. 233 (2020) 118199.
[25] V. Sharma, K.S. Ghosh, Inhibition of amyloid fibrillation and destabilization of fibrils of human γD-crystallin by direct red 80 and orange G, Int. J. Biol. Macromol. 105 (2017) 956–964.
[26] B. Ahmad, L.J. Lapidus, Curcumin prevents aggregation in α-synuclein by increasing reconfiguration rate, J. Biol. Chem. 287 (12) (2012) 9193–9199.
[27] J.A. Lima, L. Hamerski, Alkaloids as potential multi-target drugs to treat Alzheimer's disease, Studies Nat. Products Chem. 61 (2019) 301–334.
[28] M. Maiti, G.S. Kumar, Biophysical aspects and biological implications of the interaction of benzophenanthridine alkaloids with DNA, Biophys Rev 1 (3) (2009) 119–129.
[29] M. Maiti, G. Suresh Kumar, Polymorphic nucleic acid binding of bioactive isoquinoline alkaloids and their role in cancer, J. Nucleic Acids (2010), 593408.
[30] K. Bhadra, G.S. Kumar, Isoquinoline alkaloids and their binding with DNA: calorimetry and thermal analysis applications, Mini Rev. Med. Chem. 10 (2010) 1235–1247.
[31] G.S. Kumar, S. Hazra, Sanguinarine, a promising anticancer therapeutic: photochemical and nucleic acid binding properties, RSC Adv. 4 (2014) 56518–56531.
[32] A. Basu, G.S. Kumar, Nucleic acids binding strategies of small molecules: lessons from alkaloids, BBA – Gen. Subj. 1862 (9) (2018) 1995–2016.
[33] A. Basu, G.S. Kumar, Interaction of the putative anticancer alkaloid chelerythrine with nucleic acids: biophysical perspectives, Biophys. Rev. 12 (6) (2020) 1369–1386.
[34] K.C. Godowski, Antimicrobial action of sanguinarine, Int. J. Clin. Dent. 1 (1989) 96–101.
[35] G.L. Southard, R.T. Boulware, D.R. Walborn, W.J. Groznik, E.E. Thorne, S. L. Yankell, Sanguinarine, a new antiplaque agent: retention and plaque specificity, J. Am. Dent. Assoc. 108 (3) (1984) 338–341.
[36] I. Slaninová, E. Táborská, H. Bochořáková, J. Slanina, Interaction of benzo [c] phenanthridine and protoberberine alkaloids with animal and yeast cells, Cell Biol. Toxicol. 17 (2001) 51–63.
[37] V.M. Adhami, M.H. Aziz, S.R. Reagan-Shaw, M. Nihal, H. Mukhtar, N. Ahmad, Sanguinarine causes cell cycle blockade and apoptosis of human prostate carcinoma cells via modulation of cyclin kinase inhibitor-cyclin-cyclin-dependent kinase machinery, Mol. Cancer Ther. 3 (2004) 933–940.
[38] V. Simanek, R. Vespalec, A. Sedo, J. Ulrichova, J. Vicar, Quaternarybenzo(c) Phenanthridine Alkaloids–Biological Activities: Chemical Probes In Biology, Kluwer Academic Publishers, Netherlands, 2003, pp. 245–254.
[39] I. Slaninová, K. Pěnčíková, J. Urbanová, J. Slanina, E. Táborská, Antitumour activities of sanguinarine and related alkaloids, Phytochem. Rev. 13 (1) (2014) 51–68.
[40] J. Malikova, A. Zdarilova, A. Hlobilkova, Effects of sanguinarine and chelerythrine on the cell cycle and apoptosis, Biomed. Pap. 150 (1) (2006) 5–12.
[41] I. Mackraj, T. Govender, P. Gathiram, Sanguinarine, Cardiovasc. Ther. 26 (2008) 75–83.
[42] J.-J. Lu, J.-L. Bao, X.-P. Chen, M. Huang, Y.-T. Wang, Alkaloids isolated from natural herbs as the anticancer agents, J. Evid.-.based Complement. Altern. Med. (2012), 485042.
[43] R.F. Steiner, L. Weinry, Excited States of Protein and Nucleic Acid, Plenum Press, New York, 1971.
[44] Y.-Q. Wang, H.-M. Zhang, B.-P. Tang, The interaction of C.I. acid red 27 with human hemoglobin in solution, J. Photochem. Photobiol. B 100 (2) (2010) 76–83.
[45] J.R. Lakowicz (Ed.), Principles of Fluorescence Spectroscopy, Springer US, Boston, MA, 1999.
[46] J.R. Lakowicz, Principles of Fluorescence Spectroscopy, third ed., Springer Science +Business Media, New York, 2006, pp. 63–606.
[47] L. Stryer, R.P. Haugland, Energy transfer: a spectroscopic ruler, Proc. Natl. Acad. Sci. USA 58 (2) (1967) 719–726.
[48] N. Shahabadi, M. Maghsudi, Z. Kiani, M. Pourfoulad, Multispectroscopic studies on the interaction of 2-tert-butylhydroquinone (TBHQ), a food additive, with bovine serum albumin, Food Chem. 124 (3) (2011) 1063–1068.
[49] A. Basu, G. Suresh Kumar, Binding and inhibitory effect of dyes amaranth and tartrazine on amyloid fibrillation in lysozyme, J. Phys. Chem. B 121 (2017) 1222–1239.
[50] O.K. Abou-Zied, O.I.K. Al-Shihi, Characterization of subdomain IIA binding site of human serum albumin in its native, unfolded, and refolded states using small molecular probes, J. Am. Chem. Soc. 130 (32) (2008) 10793–10801.
[51] G. Zhang, Q. Que, J. Pan, J. Guo, Study of the interaction between icariin and human serum albumin by fluorescence spectroscopy, J. Mol. Struct. 881 (1-3) (2008) 132–138.
[52] J.W. Wu, K.-N. Liu, S.-C. How, W.-A. Chen, C.-M. Lai, H.-S. Liu, C.-J. Hu, S.-S. Wang, R.H. Khan, Carnosine's effect on amyloid fibril formation and induced cytotoxicity of lysozyme, PLoS ONE 8 (12) (2013) e81982.
[53] A. Kroes-Nijboer, P. Venema, J. Bouman, E. van der Linden, Influence of protein hydrolysis on the growth kinetics of β-lg fibrils, Langmuir 27 (10) (2011) 5753–5761.
[54] L. Nielsen, R. Khurana, A. Coats, S. Frokjaer, J. Brange, S. Vyas, V.N. Uversky, A. L. Fink, Effect of environmental factors on the kinetics of insulin fibril formation: elucidation of the molecular mechanism, Biochemistry 40 (2001) 6036–6046.
[55] B. Samai, A. Basu, S.S. Mati, S.C. Bhattacharya, Antiamyloid activity of functionalized cerium oxide nanoparticle on lysozyme fibrillation: spectroscopic and microscopic investigation, Materialia 6 (2019), 100285.
[56] S.W. Provencher, J. Gloeckner, Estimation of globular protein secondary structure from circular dichroism, Biochemistry 20 (1) (1981) 33–37.
[57] I.H.M. van Stokkum, H.J.W. Spoelder, M. Bloemendal, R. van Grondelle, F.C. A. Groen, Estimation of protein secondary structure and error analysis from circular dichroism spectra, Anal. Biochem. 191 (1) (1990) 110–118.
[58] N. Sreerama, R.W. Woody, Estimation of protein secondary structure from circular dichroism spectra: comparison of CONTIN, SELCON, and CDSSTR methods with an expanded reference set, Anal. Biochem. 287 (2000) 252–260.
[59] L. Whitmore, B.A. Wallace, DICHROWEB, an online server for protein secondary structure analyses from circular dichroism spectroscopic data, Nucleic Acids Res. 32 (2004) W668–W673.
[60] L. Whitmore, B.A. Wallace, Protein secondary structure analyses from circular dichroism spectroscopy: Methods and reference databases, Biopolymers 89 (2008) 392–400.
[61] A. Basu, G. Suresh Kumar, Interaction and inhibitory influence of the azo dye carmoisine on lysozyme amyloid fibrillogenesis, Mol. BioSyst. 13 (8) (2017) 1552–1564.
[62] A. Basu, S.C. Bhattacharya, G. Suresh Kumar, Influence of the ionic liquid 1-butyl-3-methylimidazolium bromideon amyloid fibrillogenesis in lysozyme: Evidence from photophysical and imaging studies, Int. J. Biol. Macromol. 107 (2018) 2643–2649.
[63] A. Basu, A. Mahammad, A. Das, Inhibition of the formation of lysozyme fibrillar assemblies by the isoquinoline alkaloid coralyne, New J. Chem. 46 (7) (2022) 3258–3269.
[64] C. Jash, G. Suresh Kumar, Chelerythrine–lysozyme interaction: spectroscopic studies, thermodynamics and molecular modeling exploration, Phys. Chem. Chem. Phys. 17 (2015) 16630–16645.
[65] K. Hayashi, T. Imoto, G. Funatsu, M. Funatsu, The position of the active tryptophan residue in lysozyme, J. Biochem. 58 (1965) 227–235.
[66] E. Nishimoto, S. Yamashita, N. Yamasaki, T. Imoto, Resolution and characterization of tryptophyl fluorescence of hen egg-white lysozyme by quenching- and time-resolved spectroscopy, Biosci. Biotechnol. Biochem. 63 (2) (1999) 329–336.
[67] G. Weber, Enumeration of components in complex systems by fluorescence spectrophotometry, Nature 190 (4770) (1961) 27–29.
[68] F.C. Wu, R.B. Mills, R.D. Evans, P.J. Dillon, Kinetics of metal−fulvic acid complexation using a stopped-flow technique and three-dimensional excitation emission fluorescence spectrophotometer, Anal. Chem. 76 (1) (2004) 110–113.

[69] J. Kang, Y. Liu, M. Xie, S. Li, M. Jiang, Y. Wang, Interactions of human serum albumin with chlorogenic acid and ferulic acid, Biochim. Biophys. Acta 1674 (2) (2004) 205–214.
[70] G.M. Morris, D.S. Goodsell, R.S. Halliday, R. Huey, W.E. Hart, R.K. Belew, A. J. Olson, Automated docking using a Lamarckian genetic algorithm and an empirical binding free energy function, J. Comput. Chem. 19 (14) (1998) 1639–1662.
[71] P.S. Vassar, C.F.A. Culling, Fluorescent stains, with special reference to amyloid and connective tissues, Arch. Pathol. 68 (1959) 487–498.
[72] Y. Kumar, S. Tayyab, S. Muzammil, Molten-globule like partially folded states of human serum albumin induced by fluoro and alkyl alcohols at low pH, Arch. Biochem. Biophys. 426 (1) (2004) 3–10.
[73] I. Nasir, M. Lundqvist, C. Cabaleiro-Lago, Size and surface chemistry of nanoparticles lead to a variant behavior in the unfolding dynamics of human carbonic anhydrase, Nanoscale 7 (41) (2015) 17504–17515.
[74] S. Bag, R. Mitra, S. DasGupta, S. Dasgupta, Inhibition of human serum albumin fibrillation by two-dimensional nanoparticles, J. Phys. Chem. B 121 (22) (2017) 5474–5482.
[75] P.J.G. Coutinho, Photophysics and biophysical applications of benzo[α] phenoxazine type fluorophores, Rev. Fluorescence (2007) 335–362.
[76] B. Bolognesi, J.R. Kumita, T.P. Barros, E.K. Esbjorner, L.M. Luheshi, D.C. Crowther, M.R. Wilson, C.M. Dobson, G. Favrin, J.J. Yerbury, ANS binding reveals common features of cytotoxic amyloid species, ACS Chem. Biol. 5 (8) (2010) 735–740.
[77] S.K. Chaturvedi, P. Alam, J.M. Khan, M.K. Siddiqui, P. Kalaiarasan, N. Subbarao, Z. Ahmad, R.H. Khan, Biophysical insight into the anti-amyloidogenic behavior of taurine, Int. J. Biol. Macromol. 80 (2015) 375–384.
[78] G. Sancataldo, V. Vetri, V. Foderà, G. Di Cara, V. Militello, M. Leone, A. Pastore, Oxidation enhances human serum albumin thermal stability and changes the routes of amyloid fibril formation, PLoS One 9 (1) (2014) e84552.
[79] Z. Islam, M.H. Ali, A. Popelka, R. Mall, E. Ullah, J. Ponraj, P.R. Kolatkar, Probing the fibrillation of lysozyme by nanoscaleinfrared spectroscopy, J. Biomol. Struct. Dyn. 39 (4) (2021) 1481–1490.
[80] K. Al Adem, S. Lukman, T.-Y. Kim, S. Lee, Inhibition of lysozyme aggregation and cellular toxicity by organic acids at acidic and physiological pH conditions, Int. J. Biol. Macromol. 149 (2020) 921–930.
[81] J. Milošević, R. Prodanović, N. Polović, On the Protein fibrillation pathway: oligomer intermediates detection using ATR-FTIR spectroscopy, Molecules 26 (2021) 970.
[82] H. Ramshini, B. Mannini, K. Khodayari, A. Ebrahim-Habibi, A.S. Moghaddasi, R. Tayebee, F. Chiti, Bis(indolyl)phenylmethane derivatives are effective small molecules for inhibition of amyloid fibril formation by hen lysozyme, Eur. J. Med. Chem. 124 (2016) 361–371.
[83] C. Jash, G. Suresh Kumar, Binding of alkaloids berberine, palmatine and coralyne to lysozyme: a combined structural and thermodynamic study, RSC Adv. 4 (2014) 12514–12525.
[84] S.-C. How, S.-M. Yang, A.i. Hsin, C.-P. Tseng, S.-S. Hsueh, M.-S. Lin, R.-Y. Chen, W.-L. Chou, S.-S. Wang, Examining the inhibitory potency of food additive fast green FCF against amyloid fibrillogenesis under acidic conditions, Food Funct. 7 (12) (2016) 4898–4907.
[85] H.R. Kalhor, M. Kamizi, J. Akbari, A. Heydari, Inhibition of amyloid formation by ionic liquids: ionic liquids affecting intermediate oligomers, Biomacromolecules 10 (2009) 2468–2475.
[86] W.-S. Wen, J.-K. Lai, Y.-J. Lin, C.-M. Lai, Y.-C. Huang, S.-S. Wang, J.-S. Jan, Effects of copolypeptides on amyloid fibrillation of hen egg-white lysozyme, Biopolymers 97 (2) (2012) 107–116.
[87] R.K. Kar, Z. Gazova, Z. Bednarikova, K.H. Mroue, A. Ghosh, R. Zhang, K. Ulicna, H.-C. Siebert, N.E. Nifantiev, A. Bhunia, Evidence for inhibition of lysozyme amyloid fibrillization by peptide fragments from human lysozyme: a combined spectroscopy, microscopy, and docking study, Biomacromolecules 17 (2016) 1998–2009.
[88] J. He, Y.u. Wang, A.K. Chang, L. Xu, N.a. Wang, X. Chong, H. Li, B. Zhang, G. W. Jones, Y. Song, Myricetin prevents fibrillogenesis of hen egg white lysozyme, J. Agric. Food Chem. 62 (39) (2014) 9442–9449.
[89] S. Millan, L. Satish, K. Bera, H. Sahoo, Binding and inhibitory effect of the food colorants Sunset Yellow and Ponceau 4R on amyloid fibrillation of lysozyme, New J. Chem. 43 (9) (2019) 3956–3968.
[90] B. Saha, S. Chowdhury, D. Sanyal, K. Chattopadhyay, G. Suresh Kumar, Comparative study of toluidine blue O and methylene blue binding to lysozyme and their inhibitory effects on protein aggregation, ACS, Omega 3 (3) (2018) 2588–2601.
[91] S. Das, S. Pahari, S. Sarmah, M.A. Rohman, D. Paul, M. Jana, A. Singha Roy, Lysozyme–luteolin binding: molecular insights into the complexation process and the inhibitory effects of luteolin towards protein modification, Phys. Chem. Chem. Phys. 21 (23) (2019) 12649–12666.
[92] F.K. Zaidi, R. Bhat, Two polyphenols with diverse mechanisms towards amyloidosis: differential modulation of the fibrillation pathway of human lysozyme by curcumin and EGCG, J. Biomol Struct Dyn. 40 (2022) 4593–4611.